

Technical Notes

TECHNICAL NOTES are short manuscripts describing new developments or important results of a preliminary nature. These Notes should not exceed 2500 words (where a figure or table counts as 200 words). Following informal review by the Editors, they may be published within a few months of the date of receipt. Style requirements are the same as for regular contributions (see inside back cover).

Antenna Configuration Effects on Thrust Performance of Miniature Microwave Discharge Ion Engine

Naoji Yamamoto,* Hirokazu Masui,[†]
Hiroshi Kataharada,[‡] and Hideki Nakashima[§]
Kyushu University, Fukuoka 816-8580, Japan

and
Yoshiyuki Takao[¶]

Oita National College of Technology, Oita 870-0152, Japan

Nomenclature

| | | |
|-----------------|---|--|
| e | = | electronic charge |
| F | = | thrust |
| g | = | acceleration of gravity |
| I_b | = | extracted ion beam current |
| I_{sp} | = | specific impulse |
| m_i | = | ion mass |
| \dot{m}_i | = | mass flow rate for ion source |
| \dot{m}_n | = | mass flow rate for neutralizer |
| P_i | = | incident microwave power |
| P_n | = | input power for neutralizer |
| P_r | = | reflected microwave power |
| V_b | = | beam voltage |
| α | = | doubly charged ion current to singly charged ion current ratio |
| γ_T | = | thrust coefficient |
| ε_c | = | ion beam production cost |
| η_t | = | thrust efficiency |
| η_u | = | propellant utilization |
| θ_b | = | beam divergence angle |

Introduction

THE adoption of small satellites, with their flexibility, short development time, and low cost, has been a breakthrough in space applications.^{1,2} Until recently, however, size restrictions have limited

the capacity of the available propulsion systems. Hence, the demand for mN-class miniature propulsion systems is expected to grow in the future.³ Miniature microwave discharge ion engines are candidates for use as miniature propulsion systems⁴ because an ion engine produces high thrust efficiency with a specific impulse of 3000–8000 s. Therefore, ion engines have already been used extensively in space missions.^{5–7} This type of miniature ion engine can also be used in small satellites, providing high specific impulse, so that missions such as Mars exploration would become possible. Furthermore, self-disposal of satellites whose missions have been completed will also be possible, eliminating destruction or retrieval costs. Miniature ion engines can also be used for precise high-stability attitude and position control in large spacecrafts, as well as for primary propulsion of microsatellites.⁸

Several studies have been conducted on the miniature ion engine.^{9,10} Wirz et al. showed good performance of a 3-cm miniature xenon ion (MiXI) thruster,⁹ that is, the propellant utilization and the ion beam production cost were 0.8 and 500 W/A, for $\dot{m} = 0.020$ mg/s. An electron bombardment-type ion source was used for ion production, so that operation time was limited by the thermionic cathode lifetime. A microwave discharge ion source would offer a potentially longer thruster lifetime than the electron bombardment type because it would be free from contamination and degradation of electron emission capacity.^{11,12}

A 30-W-class miniature ion engine has been developed for de-orbiting 100-kg-class satellites.² These missions require high specific impulse, so that the propellant utilization, ion beam production cost, thrust efficiency, and lifetime targets of this engine are 0.8, 700 W/A, 0.3, and 2000 h, respectively. The thrust performance of miniature microwave discharge ion engines has thus far been inferior to conventional ion engines, however, because of the high cost of ion production caused by poor microwave-plasma coupling as well as high losses from ion and electron collisions with the walls.¹³ This type of ion source has a magnetic tube formed by a magnetic circuit and an antenna to emit microwaves. The magnetic tube works as a virtual cathode because the trapped electrons gain energy from the microwaves by electron cyclotrons resonance (ECR) heating and ionize neutral atoms.⁵ For effective microwave-to-plasma energy transfer, the antenna must contact the ECR layer because a high electric field appears in the vicinity of the antenna. It was shown in our previous study that, using an L-shape antenna, the ion beam profile was unsymmetrical, being inclined toward the antenna side, and intense emission was locally observed near the tip of the antenna.¹⁴ Thus, antenna configuration affects plasma coupling. On the other hand, the surface recombination on the antenna also affects the performance of the ion source. Hence, the aim of this study is to investigate the effects of antenna configuration on the thrust performance of a miniature microwave discharge ion engine.

Experimental Equipment

The cross section of a 30-W-class miniature microwave discharge ion engine is shown in Fig. 1. The inner diameter is 18 mm, and the size of the engine is 50 × 50 × 30 mm. Flat square grids were used to extract the ion beam. The geometric parameters are shown in Table 1. This geometry was designed using a numerical analysis code developed by Nakano et al.¹⁵ The grid is made of molybdenum, and a mica sheet is used as an isolator between the two grids. The gap between the grids is 0.25 mm, and the ion beam diameter is 14 mm. The ion source consists of a magnetic circuit, which

Received 14 July 2005; revision received 9 November 2005; accepted for publication 13 November 2005. Copyright © 2005 by the American Institute of Aeronautics and Astronautics, Inc. All rights reserved. Copies of this paper may be made for personal or internal use, on condition that the copier pay the \$10.00 per-copy fee to the Copyright Clearance Center, Inc., 222 Rosewood Drive, Danvers, MA 01923; include the code 0748-4658/06 \$10.00 in correspondence with the CCC.

*Research Associate, Department of Advanced Energy Engineering Science, 6-1 Kasuga-Kouen, Kasuga; yamamoto@aes.kyushu-u.ac.jp. Member AIAA.

[†]Doctoral Candidate, Department of Advanced Energy Engineering Science, Graduate School of Engineering Sciences, Kasuga.

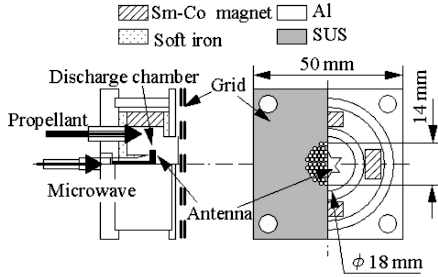
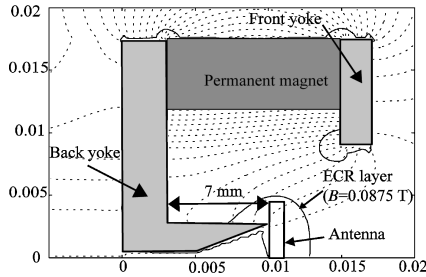
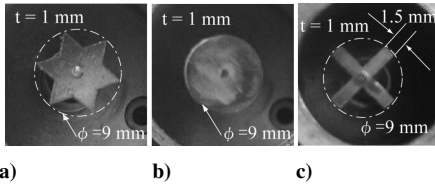
[‡]Graduate Student, Department of Advanced Energy Engineering Science, Kasuga.

[§]Professor, Department of Advanced Energy Engineering Science, Kasuga.

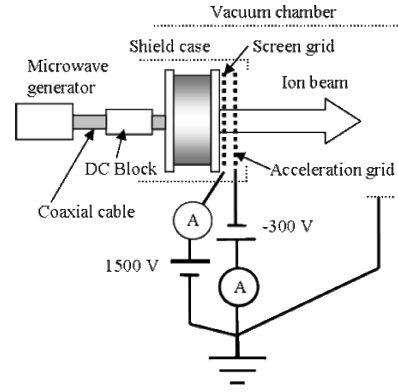
[¶]Associate Professor, Department of Electrical and Electronic Engineering, 1666 Maki; takao@oita-ct.ac.jp.

Table 1 Grid parameters

| Parameter | Screen | Acceleration |
|--------------------|------------|--------------|
| Open area ratio, % | 51 | 15 |
| Hole diameter, mm | 0.90 | 0.48 |
| Potential, V | 1500 | −300 |
| Thickness, mm | 0.30 | 0.30 |
| Hole pitch, mm | 1.20 | 1.20 |
| Material | Molybdenum | Molybdenum |
| Grid gap, mm | 0.25 | 0.25 |
| Number of holes | 121 | 121 |

**Fig. 1 Cross section of miniature ion engine developed at Kyushu University.****Fig. 2 Magnetic field profile of miniature ion engine.****Fig. 3 Photos of antennas: a) star, b) disc, and c) cross.**

has four samarium cobalt (Sm-Co) permanent magnets and iron yokes. The magnetic field profile of this engine is shown in Fig. 2. Three types of antennas—star, disc, and cross—are used, as shown in Fig. 3. The circumference of the disc antenna contacts with the ECR layer, so that good microwave-to-electron energy transfer is expected, though it has the largest surface area among three. The cross has the smallest surface area among three, though it has the narrowest contact with the ECR layer. The star antenna has small surface area and wide contact with the ECR layer. All of the antennas are inscribed in a 9-mm-diam circle and are made of molybdenum. They are 1 mm thick. The antenna lifetime of this engine might not be an important challenge because the neutralizer adopted in HAYABUSA has an antenna and demonstrated lifetime in excess of 14,000 h. The tip of the antenna is inserted into the magnetic tube formed by the magnetic circuit as shown in Fig. 2. Microwave power at 2.45 GHz was fed through a coaxial line and into an antenna. A dc block with a loss of 0.43 dB at 2.45 GHz was inserted to protect the microwave amplifier, as shown in Fig. 4. The screen grid and ion source were biased to +1500 V with respect to ground, and the acceleration grid was set to −300 V. The extracted ion beam was estimated as the current through the screen power supply minus the current through the accelerator power supply. The validity

**Fig. 4 Schematic of electric circuit.**

of this method was shown in our previous study.¹³ A neutralizer was not used in this study, as there is little difference between the extracted ion beam current without a neutralizer and that with a filament neutralizer ($\phi = 0.2 \times 100$ mm, 2% thoriated tungsten). There are several candidates for the neutralizer of this engine, including a field emission cathode,^{16,17} a filament cathode, a internal conduction cathode,¹⁸ and a microwave discharge cathode.¹⁹ A miniature microwave discharge neutralizer is under development, although it has thus far shown poor performance,¹² with an electron current of 15 mA for $P_n = 10$ W and Ar mass flow rate = 0.003 mg/s.

Pure xenon gas (99.999% pure) was used as the propellant. A thermal mass flow controller (full scale = 3 sccm) with a flow accuracy of $\pm 0.7\%$ of rate and $\pm 0.2\%$ F.S. was used. A 0.6-m-diam \times 1-m-long vacuum chamber was used in the experiments. The pumping system comprised a cryopump and a turbomolecular pump. The background pressure was maintained below 1.2×10^{-3} Pa for most of the operating conditions.

Results and Discussion

To evaluate the performance of the ion engine, ion beam production cost ε_c , propellant utilization η_u , thrust F , specific impulse I_{sp} , and thrust efficiency η_t are defined as

$$\varepsilon_c = \frac{(P_i - P_r)}{I_b} \quad (1)$$

$$\eta_u = \frac{I_b}{(e/m_i) \cdot (\dot{m}_n + \dot{m}_i)} \quad (2)$$

$$F = \gamma_T I_b \sqrt{\left(\frac{2m_i V_b}{e} \right)} \quad (3)$$

$$I_{sp} = \frac{F}{[(\dot{m}_n + \dot{m}_i)g]} \quad (4)$$

$$\eta_t = \frac{\gamma_T^2 \eta_u}{1 + \varepsilon_c/V_b + P_n/I_b V_b} \quad (5)$$

Considering the exhaust-beam divergence and the effect of doubly charged ion, γ_T is defined as

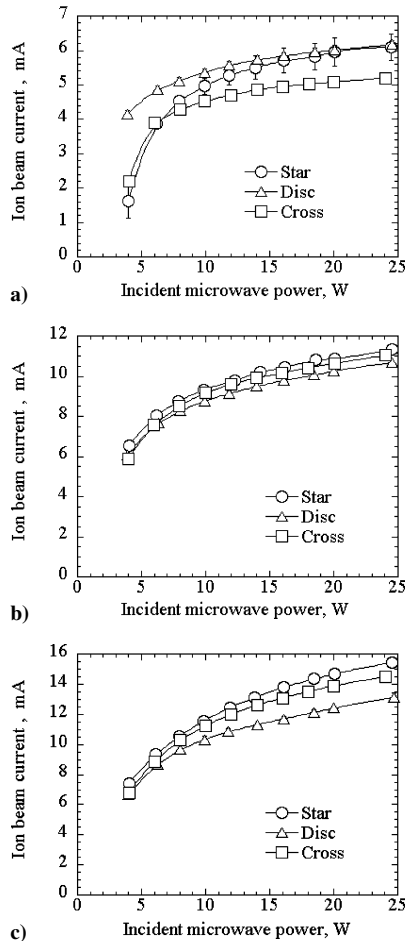
$$\gamma_T = \frac{\cos \theta_b \times (1 + \alpha/\sqrt{2})}{(1 + \alpha)} \quad (6)$$

α and θ_b are assumed to be 0.15 and 10 deg,^{20,21} respectively. Thus, in this study γ_T is estimated as $\gamma_T \approx 0.98 \cdot 0.96 = 0.94$, and \dot{m}_n and P_n are estimated as 0.003 mg/s and 10 W, respectively.

Figure 5 shows the relation between incident microwave power and ion beam current for the three antenna configurations. For $P_i = 10$ W, the ion beam currents of the disc, star, and cross configurations are 5.4, 5.0, and 4.5 mA, respectively. That is, the ion beam current of the disc antenna is the largest among the three configurations, and that of the cross antenna is the smallest for $\dot{m} = 0.01$ mg/s. On the other hand, for $P_i = 14$ W, and $\dot{m} = 0.029$ mg/s, the ion beam

Table 2 Antenna parameters

| Antenna shape | Disc | Star | Cross |
|--|----------|------|-------|
| Surface area, mm ² | 64 | 35 | 24 |
| Number of points in contact with ECR layer | ∞ | 6 | 4 |

**Fig. 5** Engine performance for different levels of ion production: a) $\dot{m} = 0.010$ mg/s, b) $\dot{m} = 0.020$ mg/s, and c) $\dot{m} = 0.029$ mg/s and $V_b = 1500$ V.

currents of the disc, star, and cross are 11.3, 13.1, and 12.6 mA, respectively. That is, for $\dot{m} = 0.020$ mg/s or $\dot{m} = 0.029$ mg/s, the ion beam current of the star antenna is the largest among the three configurations, and that of the disc antenna is the smallest. This reversal is caused by the tradeoff between the coupling of plasma with microwave and the surface recombination on the antenna: the disc antenna has the widest contact with the ECR layer, where the microwave power is absorbed efficiently,²² and it has the largest surface area among three, where the loss of ions and electrons occurs, as shown in Table 2. Therefore, under low mass flow rate, with low plasma density, the effect of good coupling with plasma exceeds the effect of large losses on the antenna surface. On the other hand, under high mass flow rate, the effect of large losses on the antenna surface exceeds the effect of good coupling with plasma. Figure 6 shows the reflection coefficient in terms of power for the three antennas. Reflection coefficient is defined as P_r/P_i . For $P_i = 10$ W, the reflection coefficient of the disc, star, and cross antennas are 0.026, 0.035, and 0.040, respectively. That is, the reflection coefficient of the disc antenna is the smallest among the three, and that of the cross antenna is the largest. This tendency can be seen for three flow rates. These results showed that the plasma-microwave coupling of the disc antenna is the best of all, and that of the cross is the worst, as mentioned earlier.

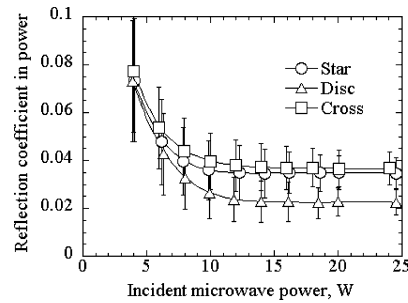
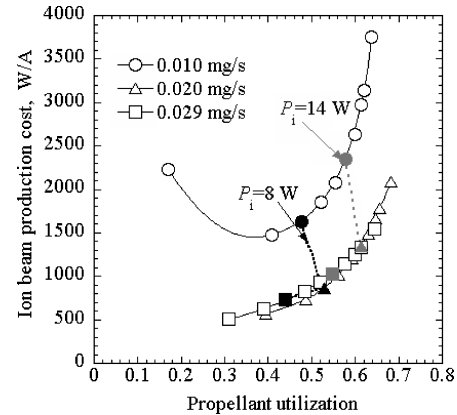
**Fig. 6** Reflection coefficient in terms of power for three antennas: $\dot{m} = 0.02$ mg/s, and $V_b = 1500$ V.**Fig. 7** Engine performance of star antenna for three flow rates: $V_b = 1500$ V, $\dot{m}_n = 0.003$ mg/s, and $P_n = 10$ W.

Figure 7 shows the engine performance of the star antenna for three flow rates. The propellant utilization decreases with an increase in mass flow rate for a given level of power because specific energy decreases with an increase in mass flow rate. Though ion beam production cost decreases with an increase in propellant utilization below 0.4 for at $\dot{m} = 0.01$ mg/s, this would be because of the low microwave-plasma coupling. Indeed, the reflection coefficient in power is 0.095 in this condition. The thrust performance parameters of the miniature ion engine, that is, η_u , ε_C , F , I_{sp} , and η_t are 0.56, 1000 W/A, 0.56 mN, 2.5×10^3 s, and 0.21, respectively at $\dot{m} = 0.02$ mg/s and $P_i = 10$ W. For practical applications, some improvement in the performance of the ion engine and drastic improvement of the neutralizer are needed. In addition, lightweight, efficient microwave power supplies are also required for practical use.

Conclusions

The effects of antenna configuration on the thrust performance of a 30-W-class miniature microwave discharge ion engine were investigated. The ion beam currents were measured for three different antenna configurations: disc, star, and cross. The results showed that the optimum antenna shape depends on the desired mass flow level because of the tradeoff between microwave-plasma coupling efficiency and surface-area recombination. For the configurations tested, the disc antenna is the best at low mass flow, whereas the star is the best at high mass flow. Overall, the thruster performance, propellant utilization efficiency, ion beam production cost, estimated thrust, estimated specific impulse, and estimated thrust efficiency are 0.56, 1000 W/A, 0.56 mN, 2500 s, and 0.21, respectively, at $\dot{m} = 0.020$ mg/s and $P_i = 10$ W.

Acknowledgments

The present work was supported by a Grant-in-Aid for Scientific Research (C)(2), No. 16560691, and a Grant-in-Aid for Young Scientists (B), No. 17760638, sponsored by The Japan Society for the Promotion of Science.

References

- ¹Kato, M., Takayama, S., Nakamura, U., Yoshihara, K., and Hashimoto, H., "Road Map of Small Satellite in JAXA," *Proceedings of the International Astronautics Congress*, Paper 05.B5.6.B.01, Oct. 2005.
- ²Sahara, H., Nakasuka, S., and Kobayashi, C., "Propulsion System for Panel Extension Satellite (PETSAT)," AIAA Paper 2005-3956, July 2005.
- ³Mueller, J., "Thruster Options for Microspacecraft: A Review and Evaluation of State-of-the Art and Emerging Technologies," *Micropropulsion for Small Spacecraft*, edited by M. M. Micci and A. D. Ketsdever, Progress in Astronautics and Aeronautics, Vol. 187, AIAA, Reston, VA, 2000, pp. 45–137.
- ⁴Mueller, J., Marrese, C., Polk, J., Yang, E., Green, A., White, V., Bame, D., Chadrabarty, I., and Vargo, S., "An Overview of MEMS-Based Micropropulsion Development at JPL," *Acta Astronautica*, Vol. 52, Nos. 9–12, 2003, pp. 881–895.
- ⁵Funaki, I., Kuninaka, H., and Toki, K., "Plasma Characterization of a 10-cm Diameter Microwave Discharge Ion Thruster," *Journal of Propulsion and Power*, Vol. 20, No. 4, 2004, pp. 718–726.
- ⁶Sovey, J. S., Rawlin, V. K., and Patterson, M. J., "Ion Propulsion Development Projects in U.S.: Space Electric Rocket Test I to Deep Space I," *Journal of Propulsion and Power*, Vol. 17, No. 3, 2001, pp. 517–526.
- ⁷Kitamura, S., Nagano, H., Nakamura, Y., Kudo, I., and Machida, K., "ETS-III Ion Engine Flight Operations in the Extended Mission Period," *Journal of Propulsion and Power*, Vol. 2, No. 6, 1986, pp. 513–520.
- ⁸Kilter, M., "Micropropulsion Technology Assessment for DAWIN," Master's Thesis, Dept. of Space Science, Luleå Univ. of Technology, Kiruna, Sweden, June 2004.
- ⁹Wirz, R. E., "Discharge Plasma Processes of Ring-Cusp Ion Thrusters," Ph.D. Dissertation, California Inst. of Technology, Pasadena, April 2005.
- ¹⁰Mistoco, V., Bilén, S., and Micci, M., "Development and Chamber Testing of a Miniature Radio-frequency Ion Thruster for Microspacecraft," AIAA Paper 2004-4124, July 2004.
- ¹¹Kuninaka, H., and Satori, S., "Development and Demonstration of Cathodeless Electron Cyclotron Resonance Ion Thruster," *Journal of Propulsion and Power*, Vol. 14, No. 6, 1998, pp. 1022–1026.
- ¹²Funaki, I., Kuninaka, H., Toki, K., Shimizu, Y., Nishiyama, K., and Horiuchi, Y., "Verification Tests of Carbon-Carbon Composite Grids for Microwave Discharge Ion Thruster," *Journal of Propulsion and Power*, Vol. 18 No. 1, 2002, pp. 169–175.
- ¹³Takao, Y., Miyamoto, T., Kataharada, H., Nakashima, H., Masui, H., Kai, T., Ijiri, H., Mori, Y., and Yamamoto, N., "Development of Small-Scale Ion Thruster Utilizing Microwave Discharge Plasma," *Proceedings of the 24th International Symposium on Space Technology and Science*, edited by J. Onodera, Japan Society for Aeronautical and Space Sciences and Organizing Committee of the 24th ISTS, Tokyo, 2004, pp. 161–166.
- ¹⁴Takao, Y., Masui, H., Miyamoto, T., Kataharada, H., Ijiri, H., and Nakashima, H., "Development of Small-Scale Microwave Discharge Ion Thruster," *Vacuum*, Vol. 73, No. 3-4, 2003, pp. 449–454.
- ¹⁵Nakano, M., Tachibana, T., and Arakawa, Y., "A Scaling Law of the Life Estimation of the Three-Grid Optics for an Ion Engine," *Transactions of the Japan Society for Aeronautical and Space Sciences*, Vol. 45, No. 149, 2002, pp. 154–161.
- ¹⁶Okawa, Y., Kitamura, S., Kawamoto, S., Iseki, Y., Hashimoto, K., and Noda, E., "An Experimental Study On Carbon Nanotube Cathodes for Electrodynamic Tether Propulsion," *Proceedings of the International Astronautics Congress*, Paper 05-C4.4.07, Oct. 2005.
- ¹⁷Yamamoto, A., Nakai, H., Kaneko, N., Nakashizu, T., Ohsawa, S., Sugimura, T., and Ikeda, M., "The Research on the Carbon Nano Tube Cathode," *Proceedings of the 2003 Particle Accelerator Conference*, Vol. 5, IEEE Computer Society, Washington, DC, 2003, pp. 3326–3328.
- ¹⁸Wirz, R., Gale, M., Mueller, J., and Marrese, C., "Miniature Ion Thrusters for Precision Formation Flying," AIAA Paper 2004-4115, July 2004.
- ¹⁹Tanisho, M., Kataharada, H., Yamamoto, N., and Nakashima, H., "A Miniaturized Ion Thruster and Neutralizer with Microwave Discharge," *Proceedings of the International Astronautics Congress*, Paper 05-CIAC-05-C4.4.02, Oct. 2005.
- ²⁰Satori, S., Kuninaka, H., and Otaki, M., "Beam Diagnostics of a Microwave Discharge Ion Engine," *The Japan Society for Aeronautical and Space Sciences*, Vol. 46, No. 534, 1998, pp. 406–412 (in Japanese).
- ²¹Takegahara, H., Kasai, Y., Gotoh, Y., Miyazaki, K., Hayakawa, Y., Kitamura, S., Nagano, H., and Nanamura, K., "Beam Characteristics Evaluation of ETS-VI Xenon Ion Thruster," Electric Rocket Propulsion Society, Paper 93-235, Sept. 1993.
- ²²Masui, H., Tashiro, Y., Yamamoto, N., Nakashima, H., and Funaki, I., "Analysis of Electron and Microwave Behaviors in Microwave Discharge Neutralizer," *Transactions of the Japan Society for Aeronautical and Space Sciences* (to be published).